

# **Synthesis and Optical Properties Study of a Novel 3- Imidazolyl-Substituted Coumarin Molecule with Large Stokes Shift**

Zichun Zhou,<sup>\*ab</sup> Anna Zheng<sup>b</sup>, Minzhe Wang<sup>a</sup>, Yongqian Xu<sup>a</sup>, Hongjuan Li<sup>a</sup>, Yujin Li<sup>\*b</sup>,  
Shiguo Sun<sup>\*a</sup>

<sup>a</sup>Shaanxi Key Laboratory of Natural Products & Chemical Biology, College of  
Chemistry & Pharmacy, Northwest A&F University, Yangling, Shaanxi, 712100,  
People's Republic of China.

<sup>b</sup>College of Chemical Engineering, Zhejiang University of Technology,  
Hangzhou, 310014, People's Republic of China.

## Contents

1. General Information.....	I
2. General Procedure for the Synthesis of compounds 2a-2d.....	IV
3. General Procedure for the Synthesis of compounds 3a-3d.....	V
4. Spectroscopic Data for Products.....	VI
5. Figure Data for Products.....	VIII
6. Table Data for Products.....	XII
7. Copies of Product NMR Spectra.....	XV
8. References.....	XXI

## 1. General Information

### 1.1. Materials and equipment

All of the chemicals used in the current study were purchased from commercial vendors and used as received without further purification, unless otherwise noted. All solvents were purified and dried using standard methods prior to use.  $^1\text{H}$  NMR spectra were recorded on a Bruker AM 500 spectrometer with chemical shifts reported as ppm at 500 MHz (in  $\text{CDCl}_3$  TMS as the internal standard).  $^{13}\text{C}$  NMR spectra were recorded on a Bruker NMR 400 spectrometer with chemical shifts reported as ppm at 101 MHz (in  $\text{DMSO-}d_6$  TMS as the internal standard). The high-resolution mass spectra were recorded on HRLCMS (LC-30A+TripleTOF5600). The pH of the testing systems was determined by a PHS-3C pH Meter (China). All of the chemicals used in the current study were purchased from commercial vendors and used as received without further purification, unless otherwise noted. All solvents were purified and dried using standard methods prior to use. All solvents and chemical reagents purchased from commercial sources (Energy Chemical of China) are analytical grades.

### 1.2. Absorption, emission spectra and quantum yield measurement

Absorption and emission spectra were recorded using a Shimadzu UV-1750 spectrometer and a RF-6000 fluorescence spectrometer (Japan), respectively. The quantum yield (QY) of compound **3** at corresponding states was determined according to the established method<sup>1</sup>. Specially, Rhodamine 6G (QY=95% in ethanol). In order to minimize the reabsorption effects, the absorption intensity of solution in the 10 mm fluorescence cuvette was fixed between 0.02 to 0.1. The QY of compound **3** at corresponding states was calculated according to the below equation:

$$\Phi_F = \Phi_{re} \times (I_F/I_{re}) \times (A_{re}/A_F) \times (n_F/n_{re})^2$$

Where  $\Phi$  is the QY,  $I$  is the integrated area of emission spectrum,  $A$  is the absorbance and  $n$  is the refractive index of the solvent. The subscript "F" and "re" refer to the sample and the reference, respectively.

### 1.3. Fluorescence life time test

Fluorescence life time was determined using time correlated single photon counting technique<sup>2</sup>. The emission decay curve of compound **3** was performed. Decays were recorded for compound **3** with excitation wavelengths at 375 nm. The recorded for **3a**, **3b**, **3c** and **3d** with emission wavelengths in toluene at 458 nm, 467 nm, 476 nm, 453 nm, respectively. The recorded for **3a**, **3b**, **3c** and **3d** with emission wavelengths in DMSO at 514 nm, 538 nm, 554 nm, 526 nm, respectively. Decay curve was fitted using multi exponential model as the following Eq1:

$$R(t)=B_1e^{(-t/\tau_1)}+B_2e^{(-t/\tau_2)}+B_3e^{(-t/\tau_3)} \quad (1)$$

where  $R(t)$  is the intensity usually as summed to decay as the sum of individual single exponential decays,  $B_1$ ,  $B_2$  and  $B_3$  are the pre-exponential factors,  $\tau_1$ ,  $\tau_2$  and  $\tau_3$  are the decay times. The average life time ( $\tau_{ave}$ ) of compound **3** was determined by Eq2.

$$\tau_{ave}=\frac{\sum_i B_i \tau_i^2}{\sum_i B_i \tau_i} \quad (2)$$

### 1.4. Measurement and analysis of compound **3** solubility

The solubility procedure of compound **3** in four different solvents (toluene, EA, DMSO and EtOH) were determined according to the established method<sup>3,4</sup>. An excess amount of compound **3** was added to a 0.5 mL of the four solvents at room temperature under atmospheric pressure. A 0.22  $\mu$ m pore syringe filter was used to take a sample of the liquid phase. Then, the concentration was measured by UV-vis spectrometer (Shimadzu UV-1750). The absorption spectra were recorded 3 times. The maximum deviation from the average value was found to be  $\pm 5\%$ , so it was proven that this experimental technique is reliable. The external calibration curve (Fig. S4) was obtained in different solvents and used for quantification of compound **3** in different solvents. The detection wavelength of compound **3** using in our experiments was chosen at maximum absorption wavelength.

### 1.5. Calculation of pKa Value

The pKa values for compound **3** are estimated from the changes in the fluorescence intensity with various pH values by using the relationship,  $\log[(R_{\max}-R)/(R-R_{\min})]=\text{pH}-\text{pKa}$ . R is the the emission intensity for **3a** and **3b**, and the ratio of emission intensity at two wavelengths for **3c** and **3d**.  $R_{\max}$  and  $R_{\min}$  are maximum and minimum limiting values of R, respectively. The pKa value (y-intercept) is derived from the plot of pH v.s.  $\log[(R_{\max}-R)/(R-R_{\min})]$ <sup>5</sup>.

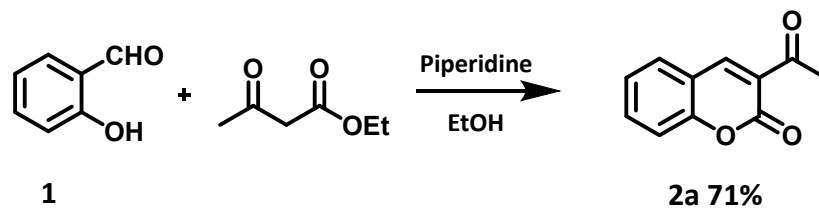
### **1.6. The measurement of lipophilicity (log P<sub>o/w</sub>)**

Lipophilicity was presented as log P<sub>o/w</sub> values, which were determined by the flask-shaking method<sup>6</sup>. The solution of compound **3** (10 μM) was partitioned in a mixture of octanol (0.5 mL) and H<sub>2</sub>O (0.5 mL). After vortexing, the mixture was centrifuged at 2000 rpm for 5 min. The octanol layer was separated from the water layer and the absorbance of both layers was measured by UV-vis spectrometer (Shimadzu UV-1750). The log P<sub>o/w</sub> was defined as the logarithmic ratio of probe concentrations in the organic and aqueous phase.

### **1.7. Theoretical calculations**

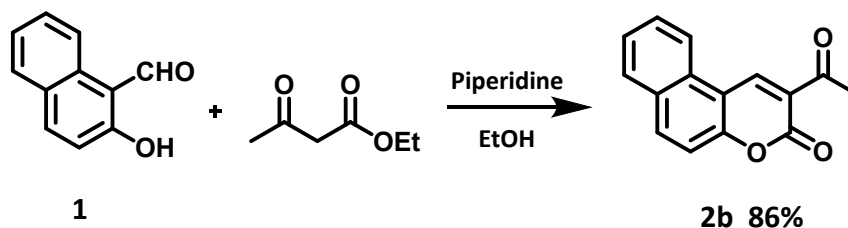
Theoretical calculations were carried out using Gaussian 16W package. The ground state (S<sub>0</sub>) and excited state (S<sub>1</sub>) geometries of the compounds were optimized using density functional theory (DFT) at the B3LYP/6-311+G(d, p) level, and the polarizable continuum model (PCM) set to toluene and DMSO. The fluorescence emission wavelength and the excitation wavelength of the compounds was investigated using time-dependent density functional theory (TD-DFT).

## **2.General Procedure for the Synthesis of compounds 2a**



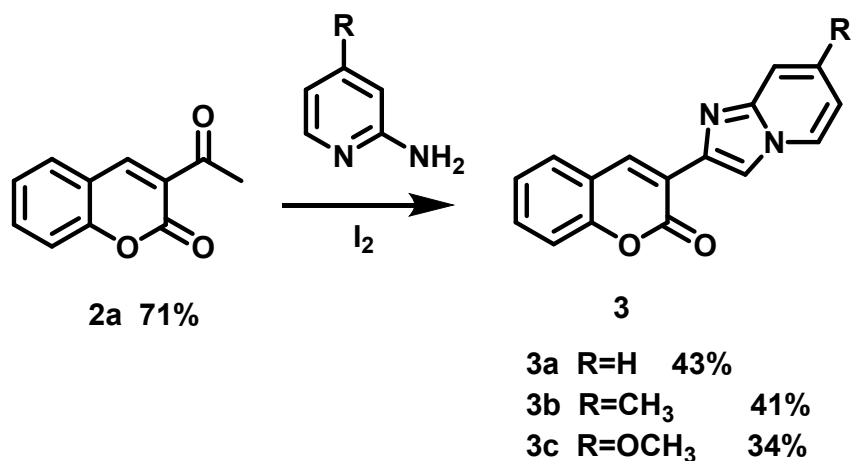
Salicylaldehyde (10 mmol, 1.2100 g), ethyl acetoacetate (10 mmol, 1.2700 g), and 0.05 mL of pyridine were added to 2.5 mL of ethanol. The mixture was refluxed at 80 °C for 4 h, and the reaction was monitored by TLC. After the reaction was complete, anhydrous ethanol was added, and the resulting solid was filtered and washed with a small amount of anhydrous ethanol to obtain crude product (yellow). The crude product was recrystallized with chloroform and petroleum ether to obtain dry white solid **2** (1.3101 g, 71%).

### 3. General Procedure for the Synthesis of compounds **2b**



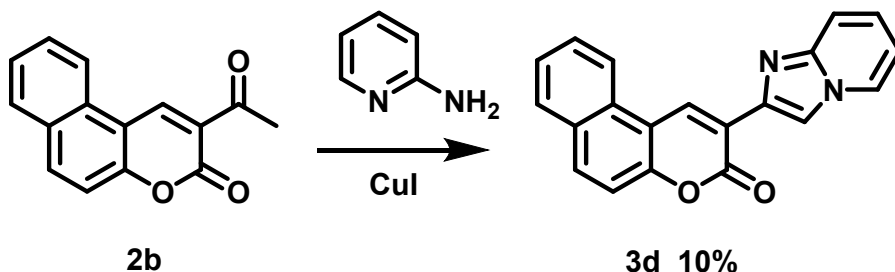
2-hydroxy-1-naphthaldehyde (10 mmol, 1.7200 g), ethyl acetoacetate (10 mmol, 1.2700 g), and 0.05 mL of pyridine were added to 2.5 mL of ethanol. The mixture was refluxed at 80 °C for 4 h, and the reaction was monitored by TLC. After the reaction was complete, anhydrous ethanol was added, and the resulting solid was filtered and washed with a small amount of anhydrous ethanol to obtain crude product (yellow). The crude product was recrystallized with chloroform and petroleum ether to obtain dry yellow solid **2** (2.0468 g, 86%).

### 3. General Procedure for the Synthesis of compounds **3a-3c**



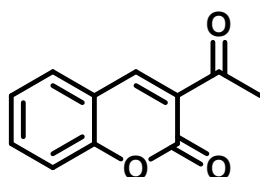
A mixture of **2a** (0.92 mmol, 0.1740 g), 2-aminopyridine (2.1 mmol, 0.1974 g), and iodine (1.0 mmol, 0.2538 g) were stirred for 2 h at 110 °C and then stirred for another 12 h at 80 °C. The residue was diluted with 2 mL of distilled water and added excess of 0.1 mL aqueous sodium hydroxide (45%). Then the reaction mixture was stirred at 100 °C for 30 min. After cooling to room temperature, the reaction mixture was diluted with 25 mL of DCM and added 10% aqueous HCl to the mixture until a neutral pH. The mixture was then extracted with DCM (30 mL×3). The organic layer was washed with water and dried with Na<sub>2</sub>SO<sub>4</sub>, and concentrated under reduced pressure. The solid was isolated by column chromatography (silica, ethyl acetate/petroleum ether 1:1 to dichloromethane/petroleum ether 3:1) to afford dark yellow solid **HP** (0.1063 g , 43%).

### 3.General Procedure for the Synthesis of compounds 3d

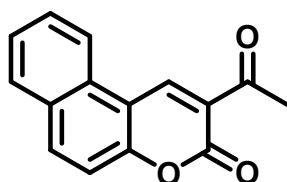


A mixture of **2b** (1.0 mmol, 0.2380 g), 2-aminopyridine (1.4 mmol, 0.1320 g), 3 mL of 1,4-dioxane as solvent and cuprous iodide (0.2 mmol, 0.038 g) were added as catalyst. The mixture was stirred at 100 °C for 14 h, cooled to room temperature, extracted with dichloromethane, the lower liquid layer was collected, and the upper liquid layer was washed with dichloromethane and repeated three times. The solid was separated by column chromatography (ethyl acetate/petroleum ether= 1:1), and the crude product was recrystallized to give yellow solid **3d** (0.0204 g, 10.0 %).

#### 4. Spectroscopic Data for Products

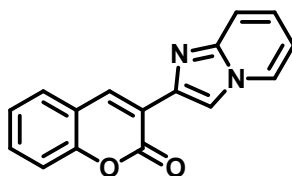


3-acetyl-2H-chromen-2-one (**2a**) White solid. Yield 71%. <sup>1</sup>H NMR (400 MHz, DMSO)  $\delta$ (ppm): 8.66 (s, 1H), 7.95 (d,  $J = 7.7$  Hz, 1H), 7.74 (q,  $J = 8.1$  Hz, 1H), 7.50–7.37 (m, 2H), 2.59 (s, 3H). <sup>13</sup>C NMR (101 MHz, DMSO)  $\delta$ (ppm): 195.54, 158.90, 155.06, 147.52, 134.94, 131.24, 125.39, 124.85, 118.61, 116.56, 30.52.

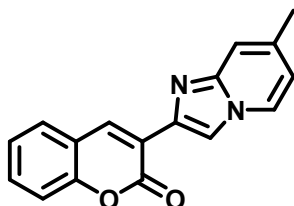


2-acetyl-3H-benzo[f]chromen-3-one (**2b**) Yellow solid. Yield 86%. <sup>1</sup>H NMR (400 MHz, DMSO)  $\delta$ (ppm): 9.28 (s, 1H), 8.63 (d,  $J = 8.4$  Hz, 1H), 8.33 (d,  $J = 9.0$  Hz, 1H), 8.09 (d,  $J = 8.0$  Hz, 1H), 7.79 (ddd,  $J = 8.3, 7.0, 1.2$  Hz, 1H), 7.70–7.60 (m, 2H), 2.66 (s, 3H). <sup>13</sup>C NMR (101 MHz, DMSO)  $\delta$ (ppm): 195.59, 158.91, 155.81, 142.94, 136.69, 130.34, 129.86, 129.59, 127.00, 123.53, 122.86, 116.93, 112.83, 30.58.

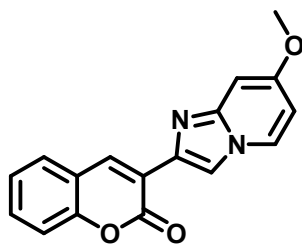




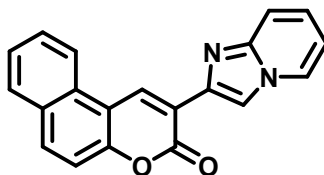
3-(imidazo[1,2-a]pyridin-2-yl)-2H-chromen-2-one (**3a**) Dark yellow solid. Yield 43%.  $^1\text{H}$  NMR (500 MHz,  $\text{CDCl}_3$ )  $\delta$ (ppm): 8.80 (s, 1H), 8.57 (s, 1H), 8.16 (d,  $J = 6.7$  Hz, 1H), 7.65 (d,  $J = 7.5$  Hz, 1H), 7.60 (d,  $J = 9.1$  Hz, 1H), 7.54 (t,  $J = 7.8$  Hz, 1H), 7.39 (d,  $J = 8.3$  Hz, 1H), 7.32 (t,  $J = 7.5$  Hz, 1H), 7.25 – 7.18 (m, 1H), 6.81 (t,  $J = 6.7$  Hz, 1H).  $^{13}\text{C}$  NMR (126 MHz,  $\text{CDCl}_3$ )  $\delta$ (ppm): 159.99, 153.10, 145.15, 138.30, 138.03, 131.32, 128.31, 126.20, 125.74, 124.67, 120.95, 119.72, 117.18, 116.42, 113.90, 112.56. HRMS (ESI)  $m/z$  calcd for  $\text{C}_{16}\text{H}_{11}\text{N}_2\text{O}_2^+(\text{M}+\text{H})^+$  263.08150, found 263.08142.



3-(7-methylimidazo[1,2-a]pyridin-2-yl)-2H-chromen-2-one (**3b**) Yellow Solid. Yield 53.6%.  $^1\text{H}$  NMR (500 MHz,  $\text{CDCl}_3$ )  $\delta$ (ppm): 8.77 (s, 1H), 8.48 (s, 1H), 8.03 (d,  $J=6.8$  Hz, 1H), 7.65 (d,  $J=7.7$  Hz, 1H), 7.53 (d,  $J=8.6$ Hz, 1H), 7.41~7.35 (m, 2H), 7.32 (t,  $J=7.6$ , 1H), 6.64 (d,  $J=6.5$  Hz, 1H), 2.42 (s, 3H).  $^{13}\text{C}$  NMR (101 MHz, DMSO)  $\delta$ (ppm): 159.41, 157.71, 152.92, 145.28, 138.00, 137.07, 131.98, 131.96, 129.28, 127.07, 125.19, 119.86, 116.37, 115.29, 114.93, 113.61, 21.40. HRMS (ESI)  $m/z$  calcd for  $\text{C}_{17}\text{H}_{13}\text{N}_2\text{O}_2^+(\text{M}+\text{H})^+$  277.09715, found 277.09702.



3-(7-methoxyimidazo[1,2-a]pyridin-2-yl)-2H-chromen-2-one (**3c**) Yellow Solid. Yield 34.0%.  $^1\text{H}$  NMR (500 MHz,  $\text{CDCl}_3$ )  $\delta$ (ppm): 8.74 (s, 1H), 8.40 (s, 1H), 7.96 (d,  $J=7.4$  Hz, 1H), 7.64 (dd,  $J=7.7, 1.3$  Hz, 1H), 7.55~7.50 (m, 1H), 7.39 (d,  $J=8.3$  Hz, 1H), 7.34~7.29 (m, 1H), 6.88 (d,  $J=2.2$  Hz, 1H), 6.54 (dd,  $J=7.4, 2.4$  Hz, 1H), 3.89 (s, 3H).  $^{13}\text{C}$  NMR (101 MHz, DMSO)  $\delta$ (ppm): 159.34, 158.66, 152.83, 146.42, 137.60, 137.49, 131.87, 129.18, 128.39, 125.16, 121.15, 119.86, 116.37, 113.12, 107.53, 94.16, 56.09. HRMS (ESI)  $m/z$  calcd for  $\text{C}_{17}\text{H}_{13}\text{N}_2\text{O}_3^+(\text{M}+\text{H})^+$  293.09207, found 293.09210.



2-(imidazo[1,2-a]pyridin-2-yl)-3H-benzo[f]chromen-3-one (**3d**) Yellow Solid. Yield 10.0%.  $^1\text{H}$  NMR (500 MHz,  $\text{CDCl}_3$ )  $\delta$ (ppm): 9.60 (s, 1H), 8.65~8.56 (m, 2H), 8.18 (d,  $J=6.7$  Hz, 1H), 7.99 (d,  $J=9.0$  Hz, 1H), 7.93 (d,  $J=8.0$  Hz, 1H), 7.73 (t,  $J=7.7$  Hz, 1H), 7.66 (d,  $J=9.0$  Hz, 1H), 7.59 (t,  $J=7.3$  Hz, 1H), 7.53 (d,  $J=9.0$  Hz, 1H), 7.24 (d,  $J=9.1$  Hz, 1H), 6.82 (t,  $J=6.6$  Hz, 1H).  $^{13}\text{C}$  NMR (101 MHz, DMSO)  $\delta$ (ppm): 166.82, 162.72, 152.63, 145.48, 133.54, 133.41, 129.46, 129.03, 126.70, 126.63, 122.64, 117.02, 117.01, 116.99, 116.96, 116.89, 114.27, 113.81, 112.81, 112.80. HRMS (ESI)  $m/z$  calcd for  $\text{C}_{20}\text{H}_{13}\text{N}_2\text{O}_2^+(\text{M}+\text{H})^+$  313.09715, found 313.09714.

## 5. Figure Data for Products

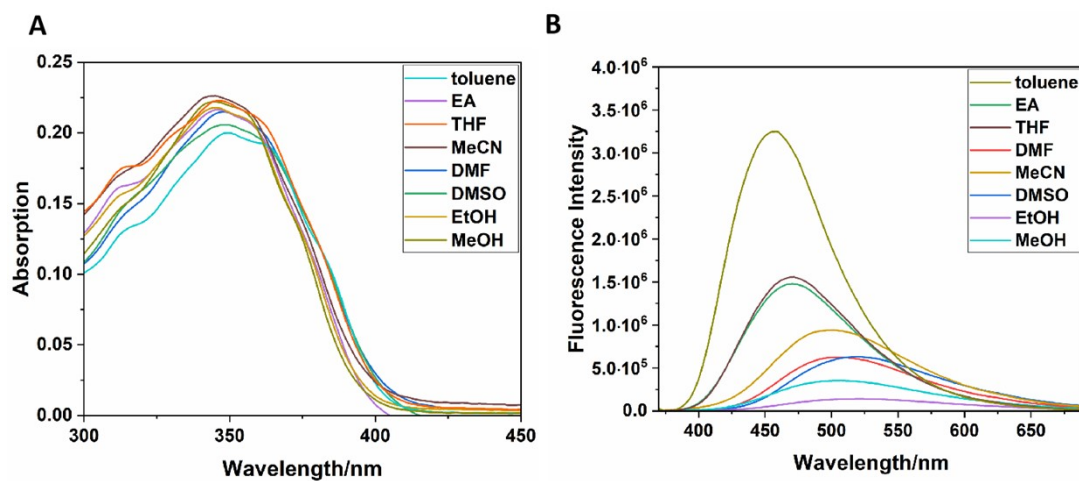


**Fig. S1** Absorption spectra (A) and fluorescence spectra (B) of compound **3a** (10  $\mu$ M,  $\lambda_{\text{ex}} = 350$  nm) in different solvents.

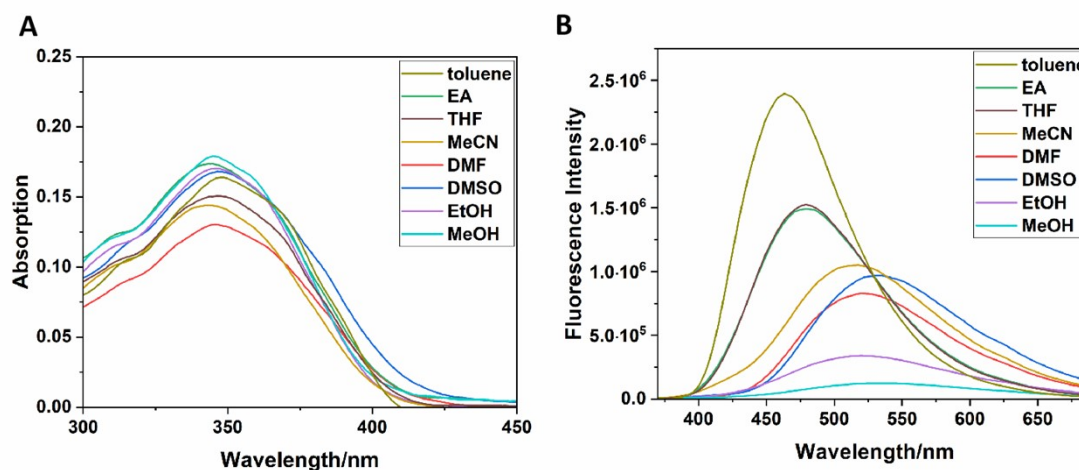


**Fig. S2** Absorption spectra (A) and fluorescence spectra (B) of compound **3b** (10  $\mu$ M,  $\lambda_{\text{ex}} = 350$  nm) in different solvents.

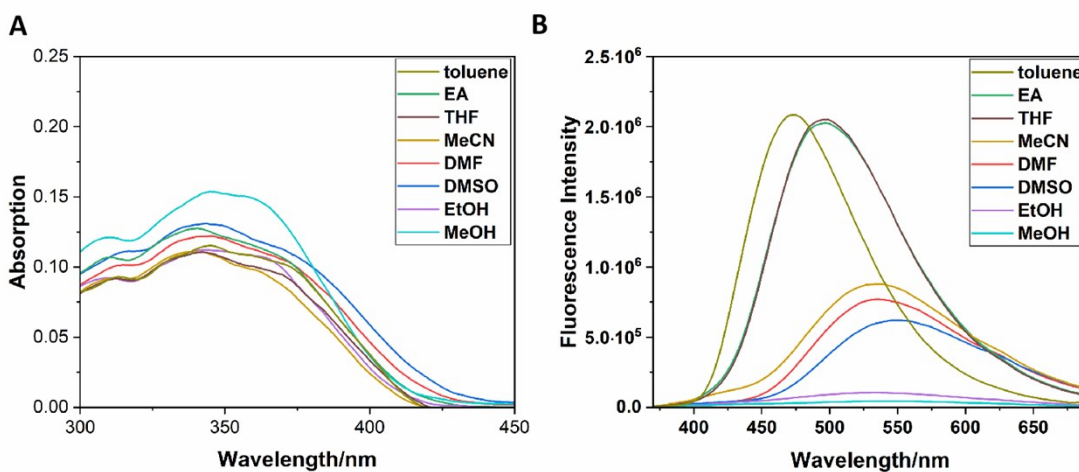


**Fig. S3** Absorption spectra (A) and fluorescence spectra (B) of compound **3c** (10  $\mu\text{M}$ ,  $\lambda_{\text{ex}} = 350 \text{ nm}$ ) in different solvents.

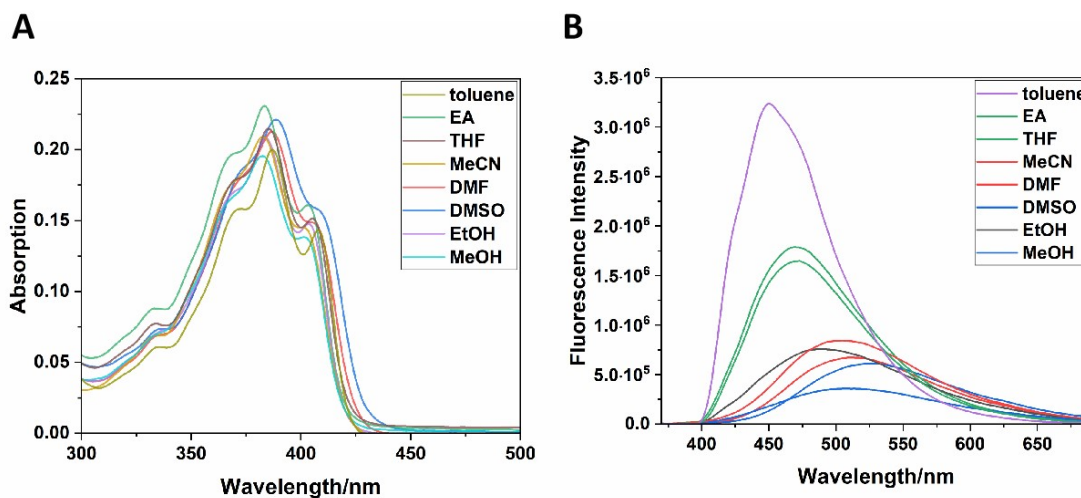


**Fig. S4** Absorption spectra (A) and fluorescence spectra (B) of compound **3d** (10  $\mu\text{M}$ ,  $\lambda_{\text{ex}} = 350 \text{ nm}$ ) in different solvents.

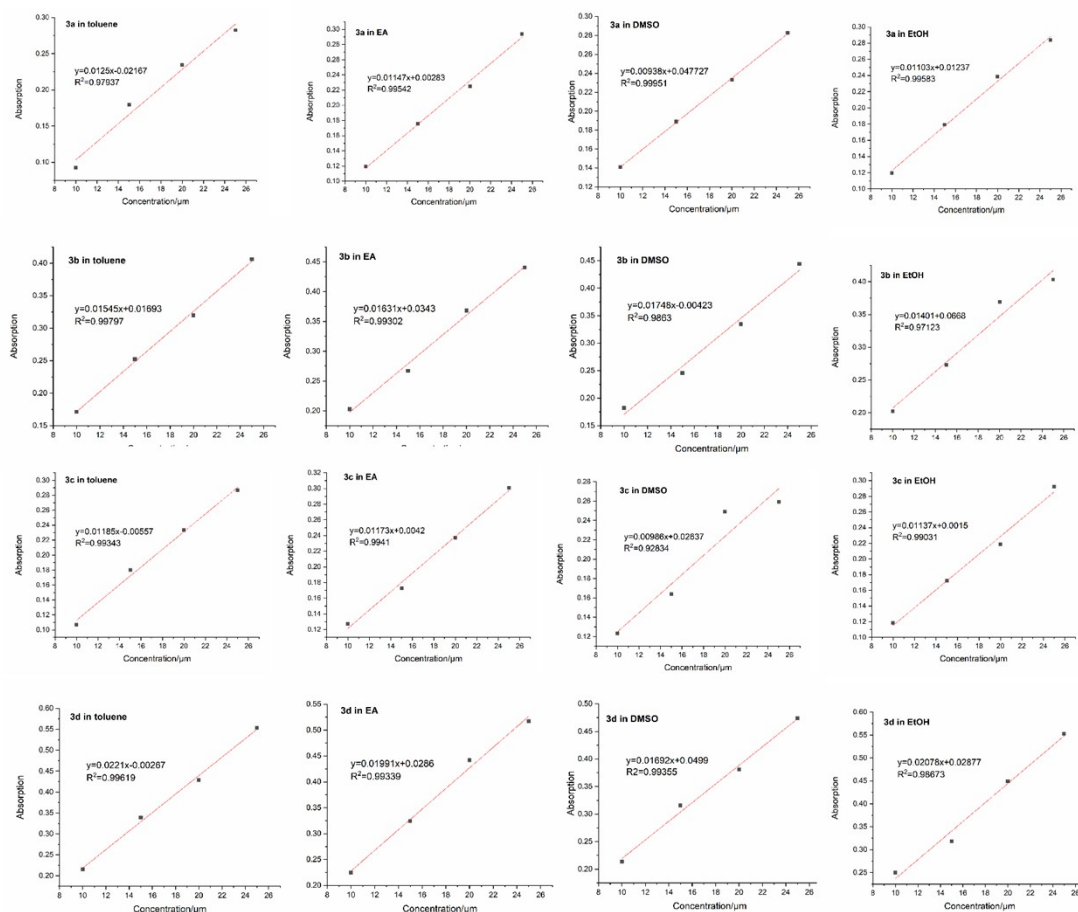


**Fig. S5** The external calibration curve (linear fitting) in different solvents of compound **3**, the concentration range were recorded at the corresponding maximum absorption wavelength.

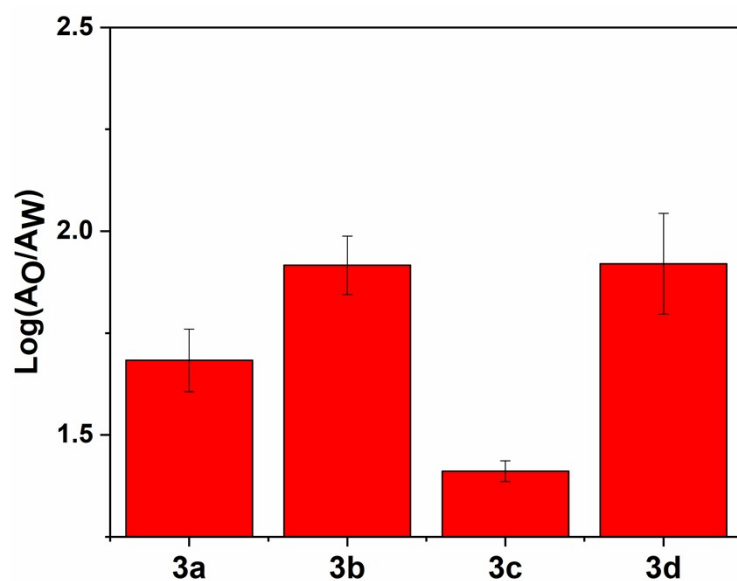


**Fig. S6** The hydrophobicity/hydrophilicity of compound **3**, measured by the determination of hydrophobicity ( $\log P_{O/W}$ ). Errors are s. d. ( $n=3$ ).

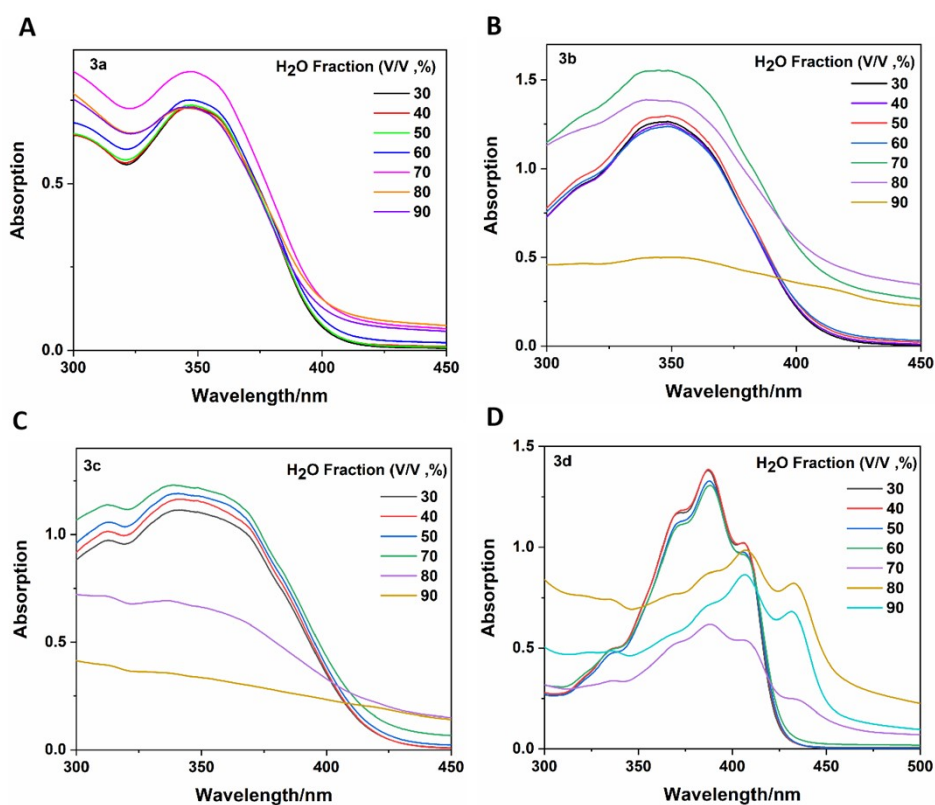


**Fig. S7** Absorption spectra and fluorescence intensity (Inset) at the excitation wavelength of 350 nm for compound **3a** (A), **3b** (B), **3c** (C) and **3d** (D) in a mixture of water-THF (V/V, %) (100  $\mu$ M).

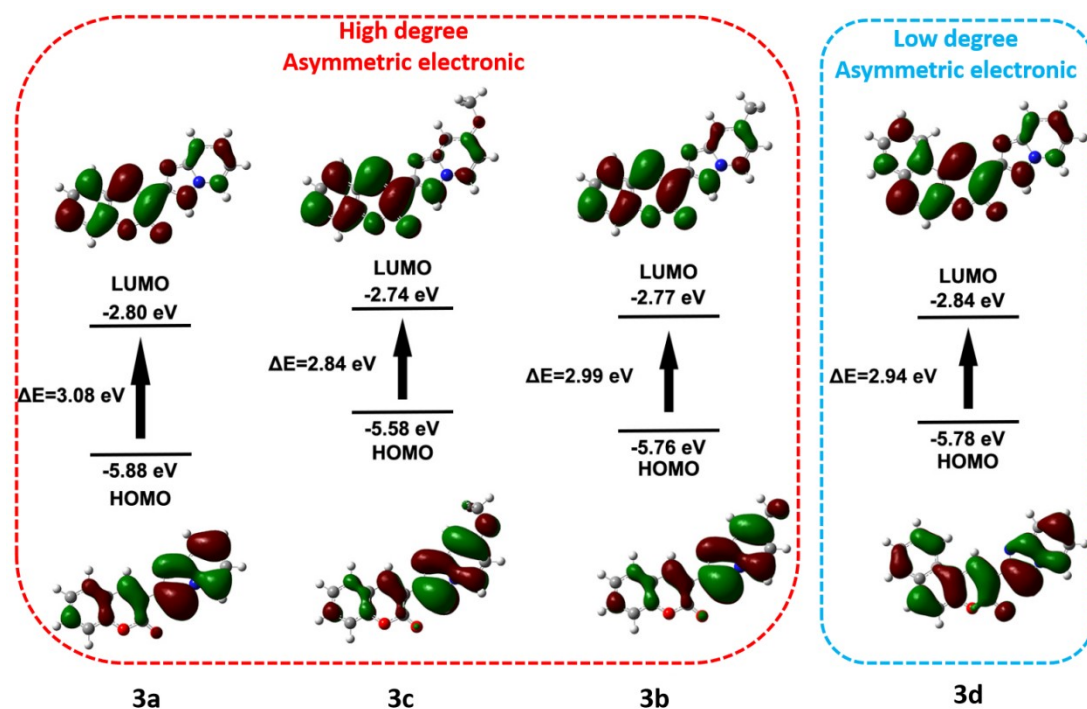


Fig. S8 Representative HOMO and LUMO diagrams of compound **3** in DMSO obtained from calculations and their corresponding energy levels

## 6. Table Data for Products

Table S1 Solubility and hydrophobicity/hydrophilicity ( $\text{Log}(A_o/A_w)$ ) of compound **3**

Compound	Solubility		$\text{Log}(A_o/A_w)$
	Solvent	Solubility (mg/mL)	
3a	toluen	162.9	1.68
	e		
	EA	180.8	
	DMSO	1157.1	
3b	EtOH	91.5	1.92
	toluen	47.9	
	e		
	EA	24.9	
3c	DMSO	101.1	1.41
	EtOH	11.5	
	toluen	28.9	
	e		
3d	EA	66.1	1.92
	DMSO	179.8	
	EtOH	18.7	
	toluen	16.0	
	e		
	EA	2.9	

DMSO	42.8
EtOH	0.9

**Table S2** Optical data of compound **3** in the solid state

Compound	$\lambda_{\text{abs}}$ (nm)	$\lambda_{\text{em}}$ (nm)	SS (nm)
<b>3a</b>	412	520	108
<b>3b</b>	383	525	142
<b>3c</b>	382	534	152
<b>3d</b>	446	520	74

**Table S3.** The IFCT analysis calculation data of compound **3**

Compound	$D^a$ (Å)	$S_r^b$	$H^c$ (Å)	$t^d$ (Å)	HDI <sup>e</sup>	EDI <sup>e</sup>
<b>3a</b>	3.963	0.52999	2.752	1.967	8.93	8.01
<b>3b</b>	4.145	0.51432	2.772	1.843	8.80	8.01
<b>3c</b>	4.278	0.50313	2.819	1.933	8.75	8.08
<b>3d</b>	1.855	0.73828	3.572	-0.954	6.60	7.16

<sup>a</sup> The total magnitude of charge transfer (CT) length between the centroid of holes and electrons; <sup>b</sup> Used to characterize the overlapping extent of holes and electrons; <sup>c</sup> The overall average distribution breadth of electrons and holes; <sup>d</sup> Used to measured separation degree of hole and electron in CT direction; <sup>e</sup> The Hole Delocalization Index (HDI) and Electron Delocalization Index (EDI): the smaller the value of HDI (EDI), the higher the degree of hole (electron) delocalization.

**Table S4.** Fluorescence decay time ( $\tau_{\text{ave}}$ ) and pre-exponential factor ( $B$ ) of compound **3**.

Dye	solvent	$\tau_1$ (ns)	$B_1$	$\chi^2$	$\tau_{\text{ave}}$ (ns)
<b>3a</b>	toluene	1.84	1532.39	0.9387	1.84
	DMSO	2.55	1447.33	1.0361	2.55
<b>3b</b>	toluene	1.80	1475.38	0.9026	1.80
	DMSO	2.84	1483.78	1.1019	2.84
<b>3c</b>	toluene	2.26	1387.59	0.9774	2.26
	DMSO	2.28	1461.20	1.0310	2.28
<b>3d</b>	toluene	1.71	1455.72	0.8651	1.71
	DMSO	1.84	1549.35	0.9160	1.84

**Table S5.** The quantum yield of compound **3** in a mixture of H<sub>2</sub>O-THF (V/V, %)

<b>Compound</b>	<b>H<sub>2</sub>O/THF</b>	<b><math>\lambda_{em}^c</math> (nm)</b>	<b><math>\Phi_F^d</math></b>
<b>3a</b>	<b>30</b>	514	0.156
	<b>40</b>	514	0.120
	<b>50</b>	517	0.090
	<b>60</b>	521	0.073
	<b>70</b>	525	0.047
	<b>80</b>	531	0.033
	<b>90</b>	536	0.019
<b>3b</b>	<b>30</b>	523	0.059
	<b>40</b>	528	0.048
	<b>50</b>	529	0.037
	<b>60</b>	531	0.027
	<b>70</b>	533	0.017
	<b>80</b>	516	0.023
	<b>90</b>	514	0.022
<b>3c</b>	<b>30</b>	530	0.062
	<b>40</b>	530	0.036
	<b>50</b>	534	0.029
	<b>70</b>	539	0.015
	<b>80</b>	478	0.042
	<b>90</b>	488	0.089
<b>3d</b>	<b>30</b>	510	0.138
	<b>40</b>	515	0.113
	<b>50</b>	516	0.101
	<b>60</b>	518	0.085
	<b>70</b>	481	0.235
	<b>80</b>	481	0.254
	<b>90</b>	489	0.198



## 7. Copies of Product NMR Spectra

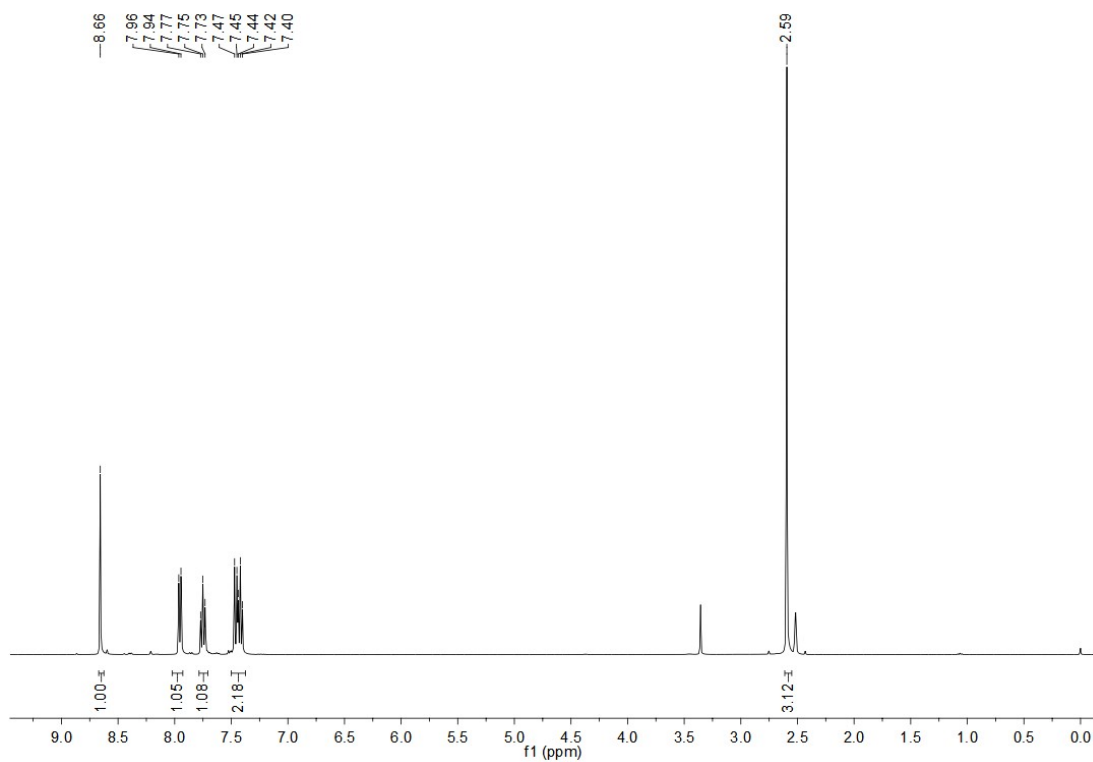


**Figure S9** The  $^1\text{H}$  NMR Spectra of 2a (400 MHz, DMSO)

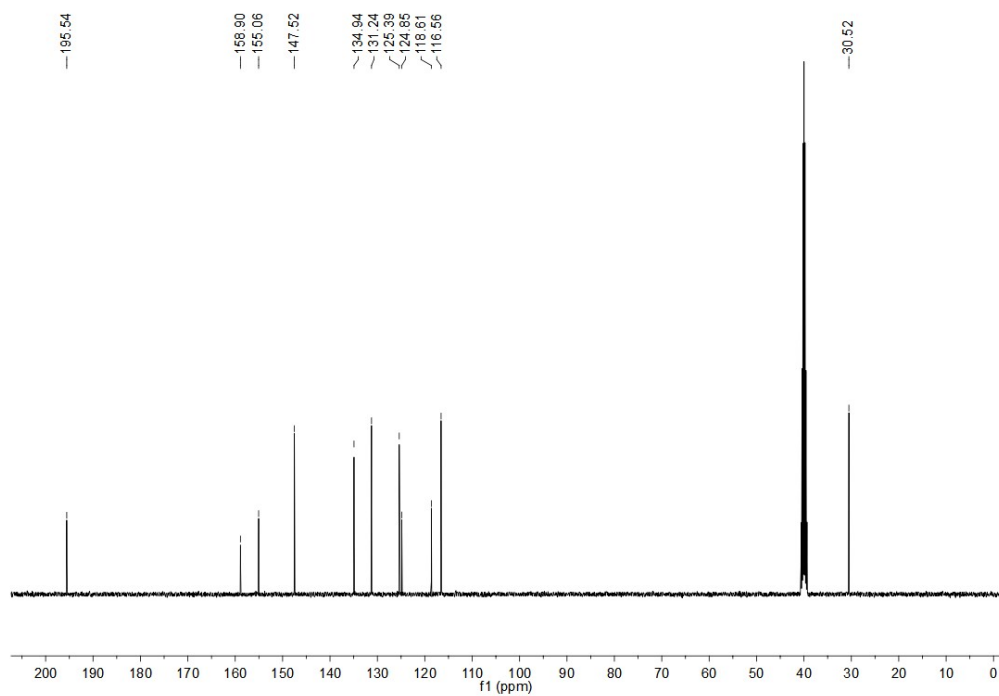


**Figure S10** The  $^{13}\text{C}$  NMR Spectra of **2a** (101 MHz, DMSO)

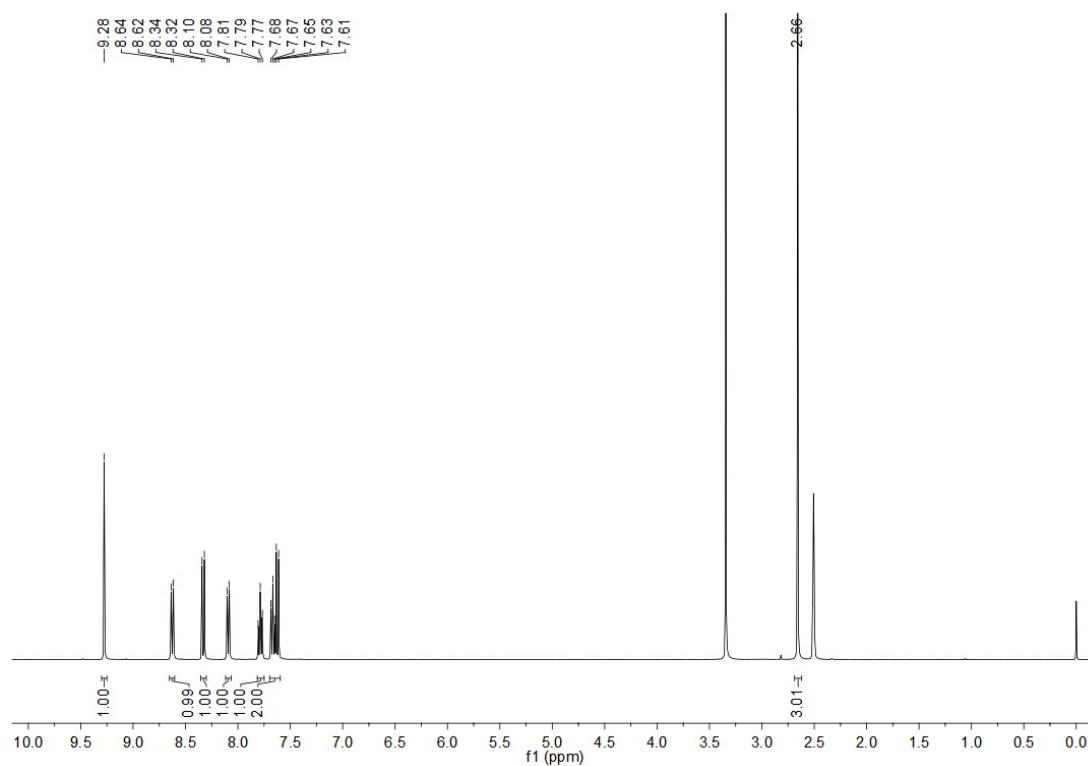


**Figure S11** The  $^1\text{H}$  NMR Spectra of **2b** (400 MHz, DMSO)

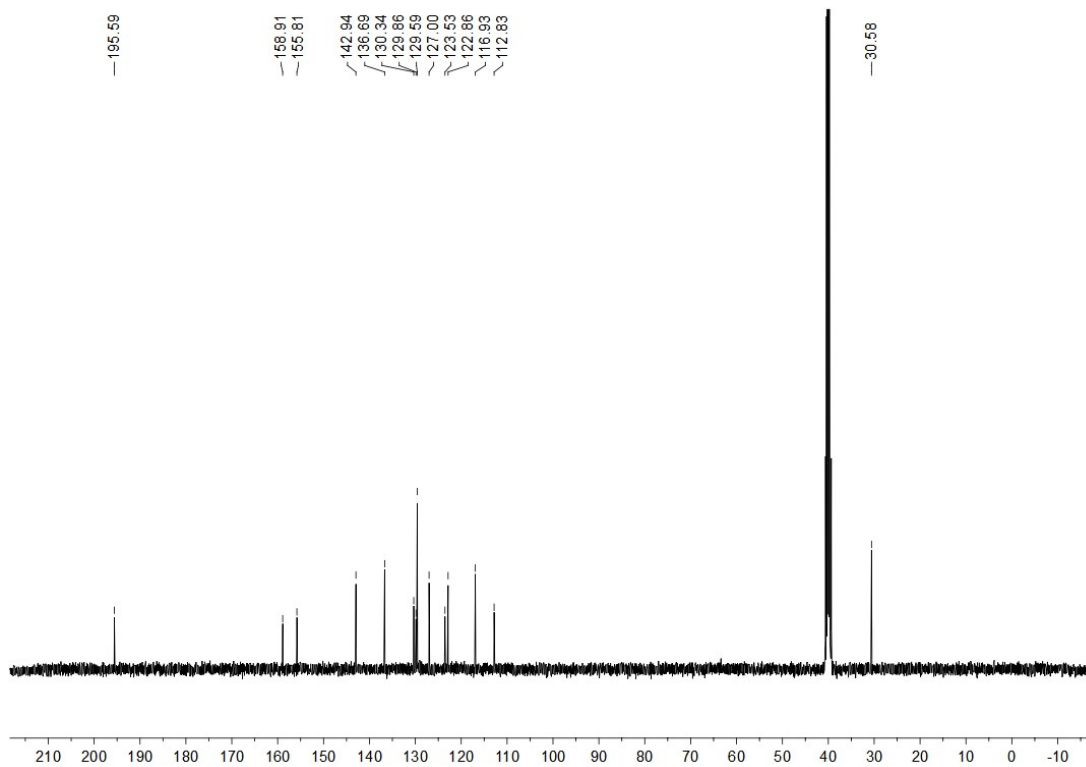


**Figure S12** The  $^{13}\text{C}$  NMR Spectra of **2b** (101 MHz, DMSO)

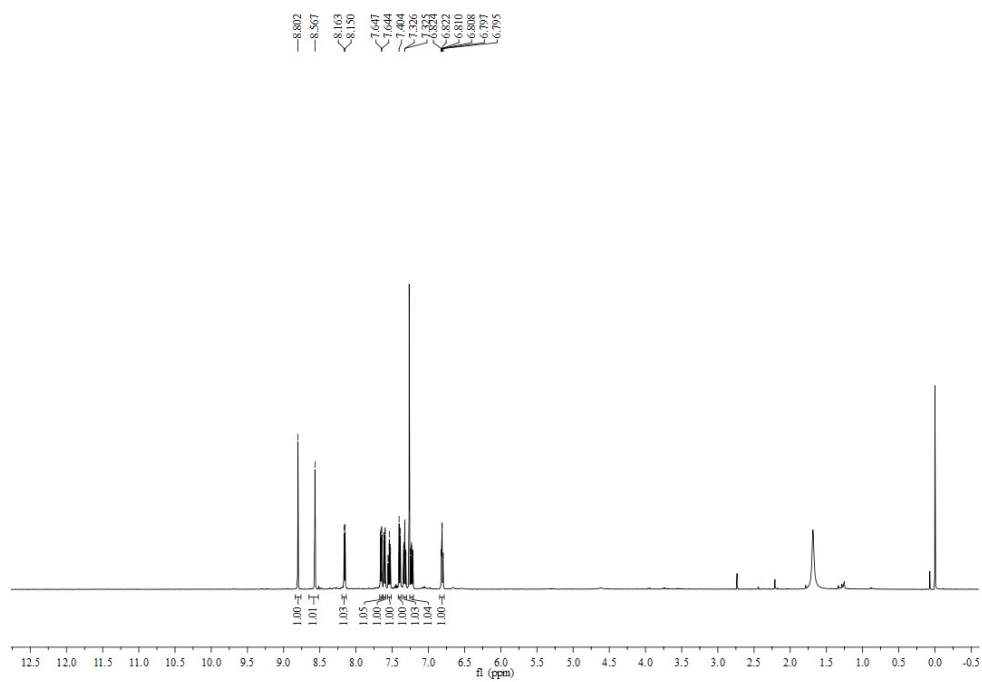


**Figure S13** The  $^1\text{H}$  NMR Spectra of **3a** (500 MHz,  $\text{CDCl}_3$ )

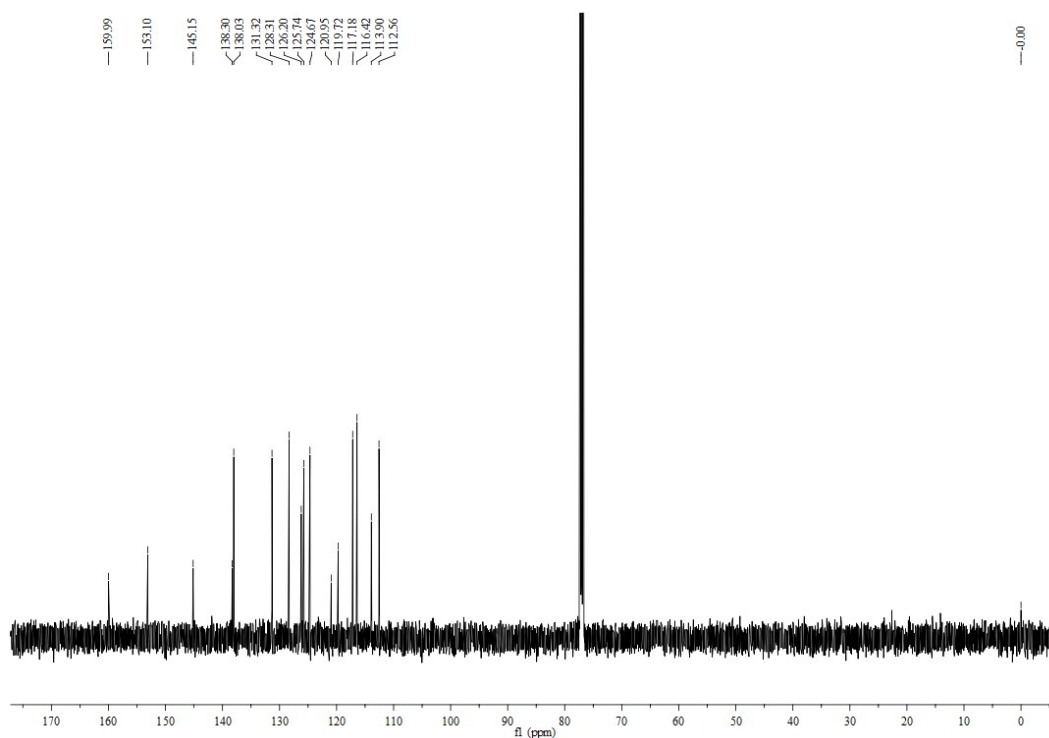


**Figure S14** The  $^{13}\text{C}$  NMR Spectra of **3a** (125 MHz,  $\text{CDCl}_3$ )

SSGZZC20230621-1 #67 RT: 0.30 AV: 1 NL: 3.30E8  
T: FTMS + p ESI Full ms [100.0000-1500.0000]

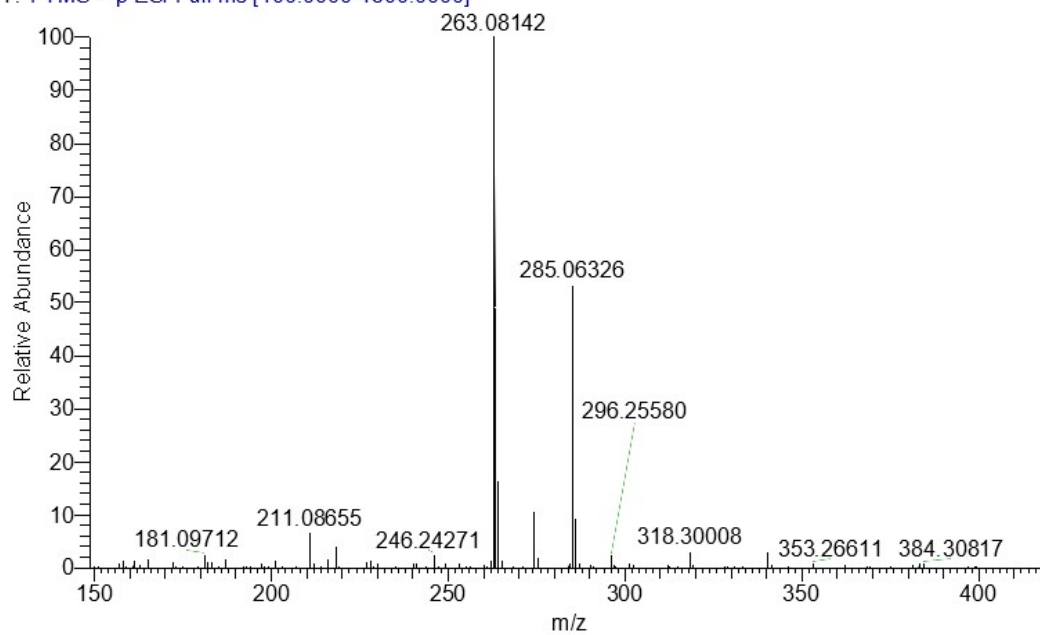


**Figure S15** The HRMS Spectra of **3a**

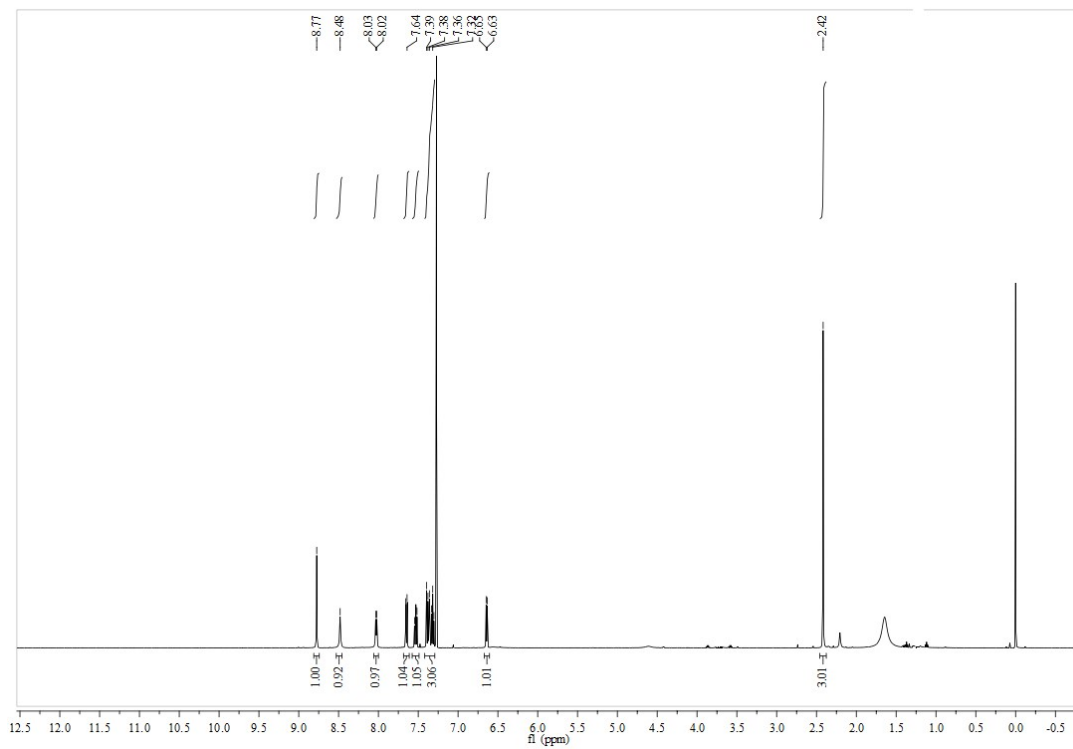


**Figure S16** The  $^1\text{H}$  NMR Spectra of **3b** (500 MHz,  $\text{CDCl}_3$ )

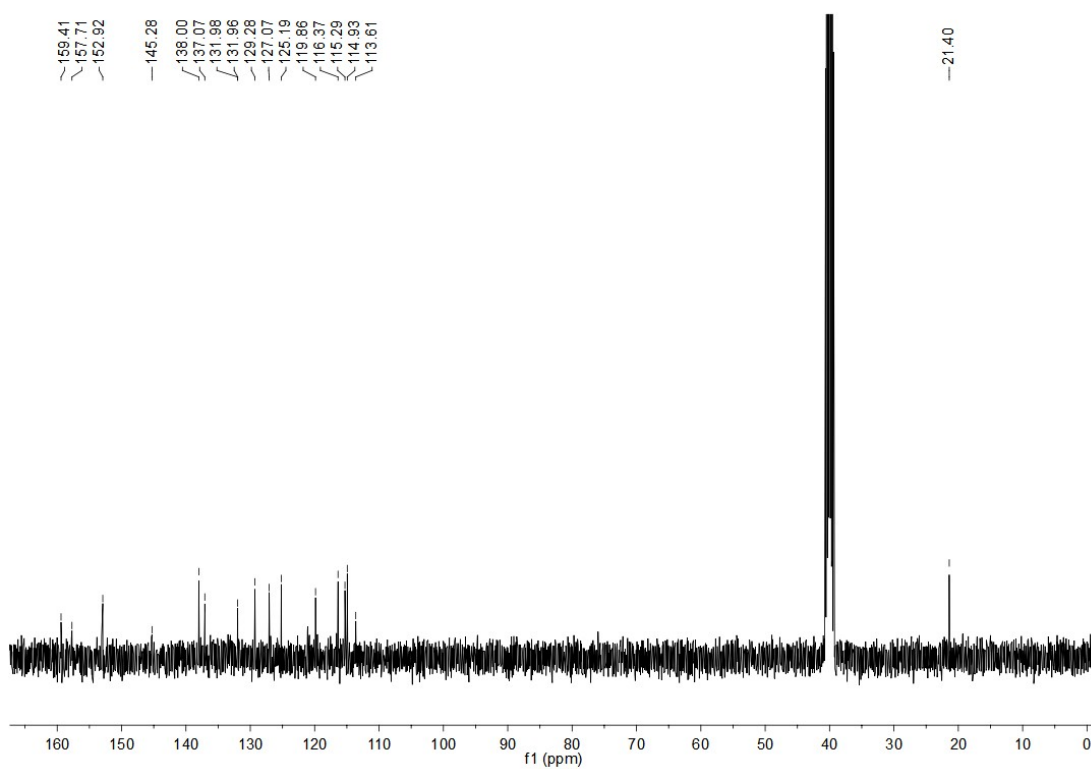


**Figure S17** The  $^{13}\text{C}$  NMR Spectra of **3b** (101 MHz, DMSO)

SSGZZC20230626-2 #159 RT: 0.71 AV: 1 NL: 1.69E8  
T: FTMS + p ESI Full ms [100.0000-1500.0000]

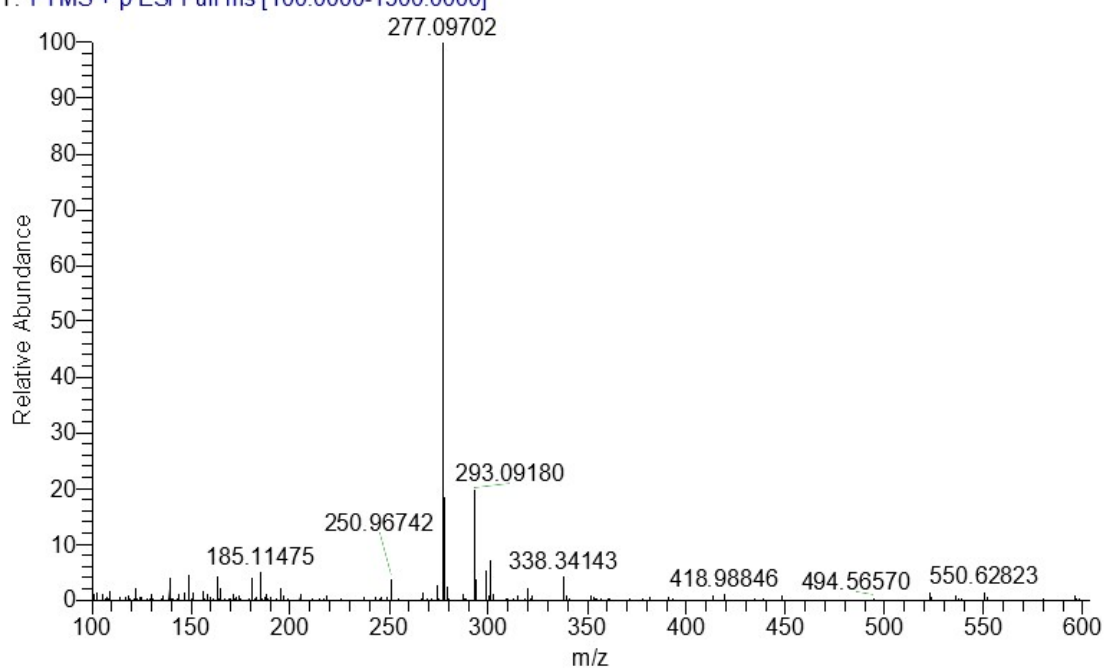


Figure S18 The HRMS Spectra of 3b

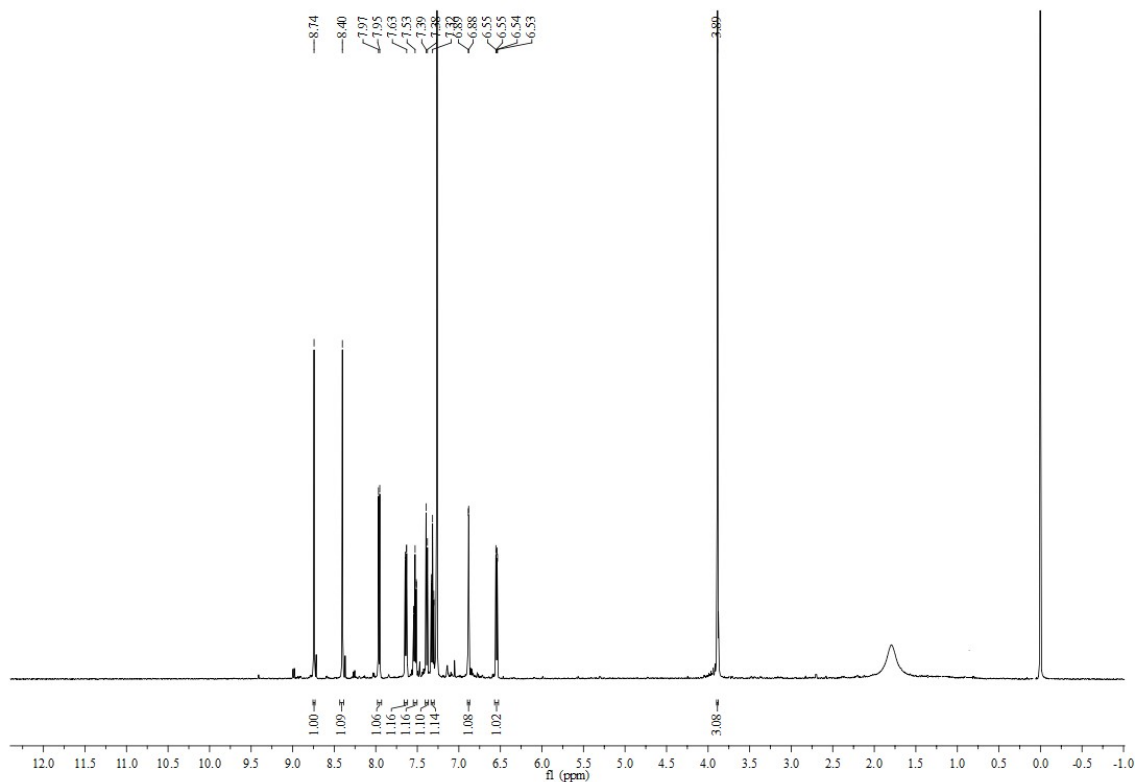
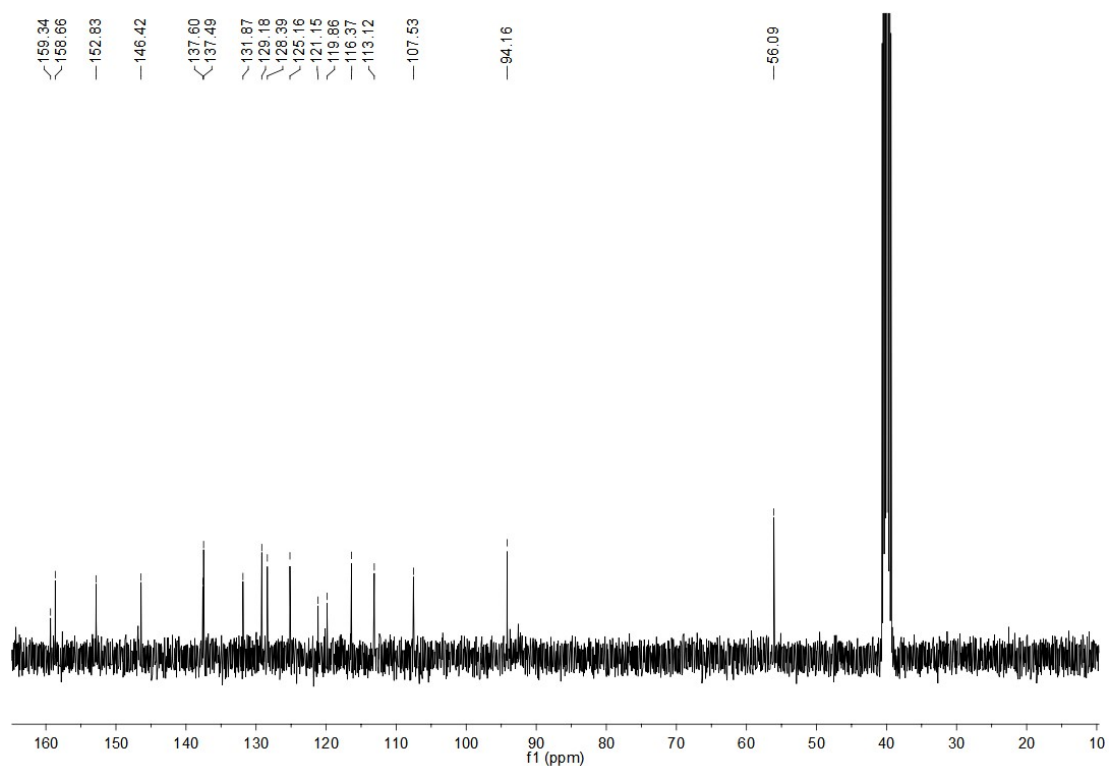
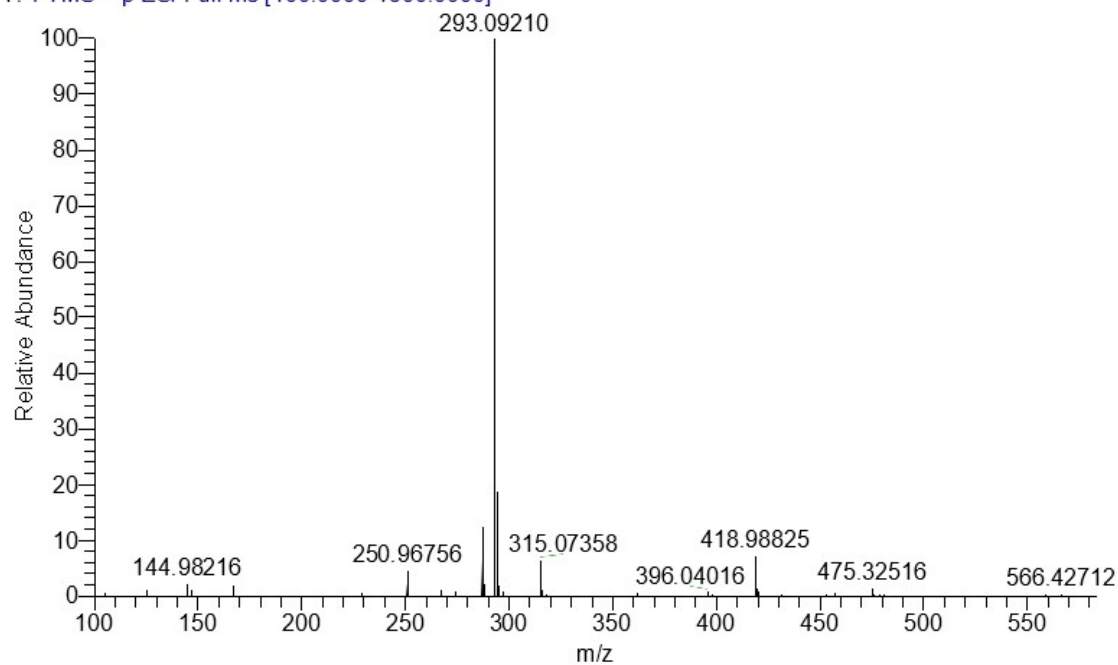


Figure S19 The  $^1\text{H}$  NMR Spectra of 3c (500 MHz,  $\text{CDCl}_3$ )



**Figure S20** The  $^{13}\text{C}$  NMR Spectra of **3c** (101 MHz, DMSO)

SSGZZC20230626-1 #24 RT: 0.11 AV: 1 NL: 1.40E9  
 T: FTMS + p ESI Full ms [100.0000-1500.0000]



**Figure S21** The HRMS Spectra of **3c**

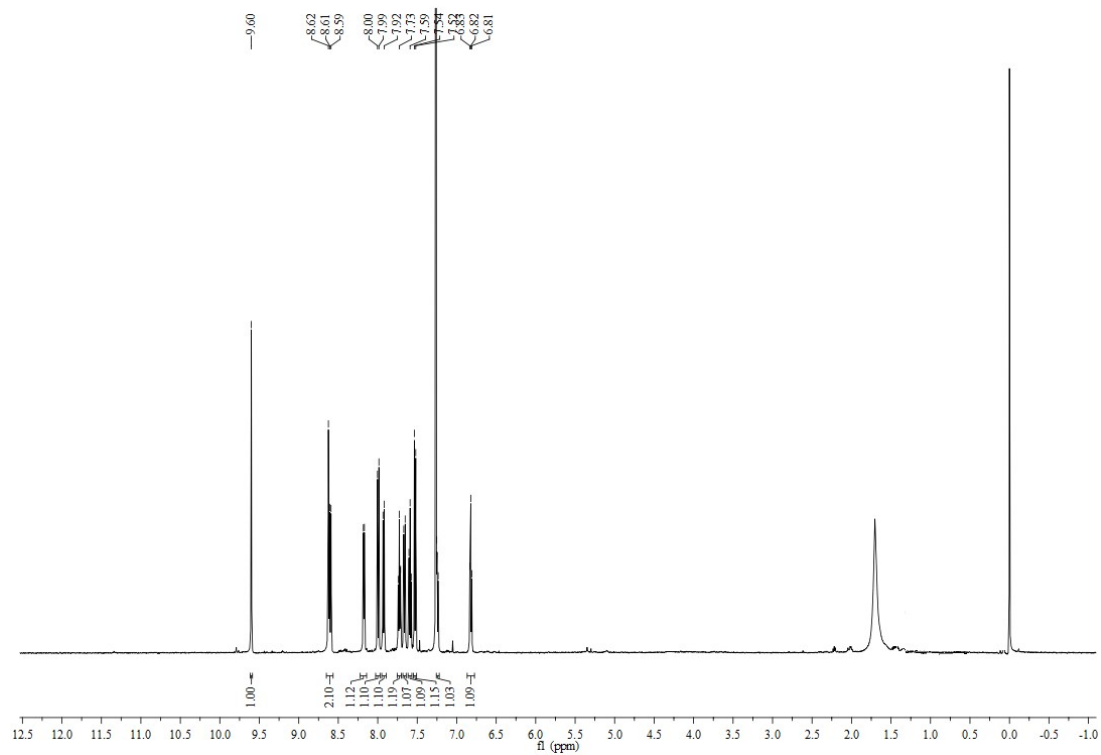


**Figure S22** The  $^1\text{H}$  NMR Spectra of **3d** (500 MHz,  $\text{CDCl}_3$ )

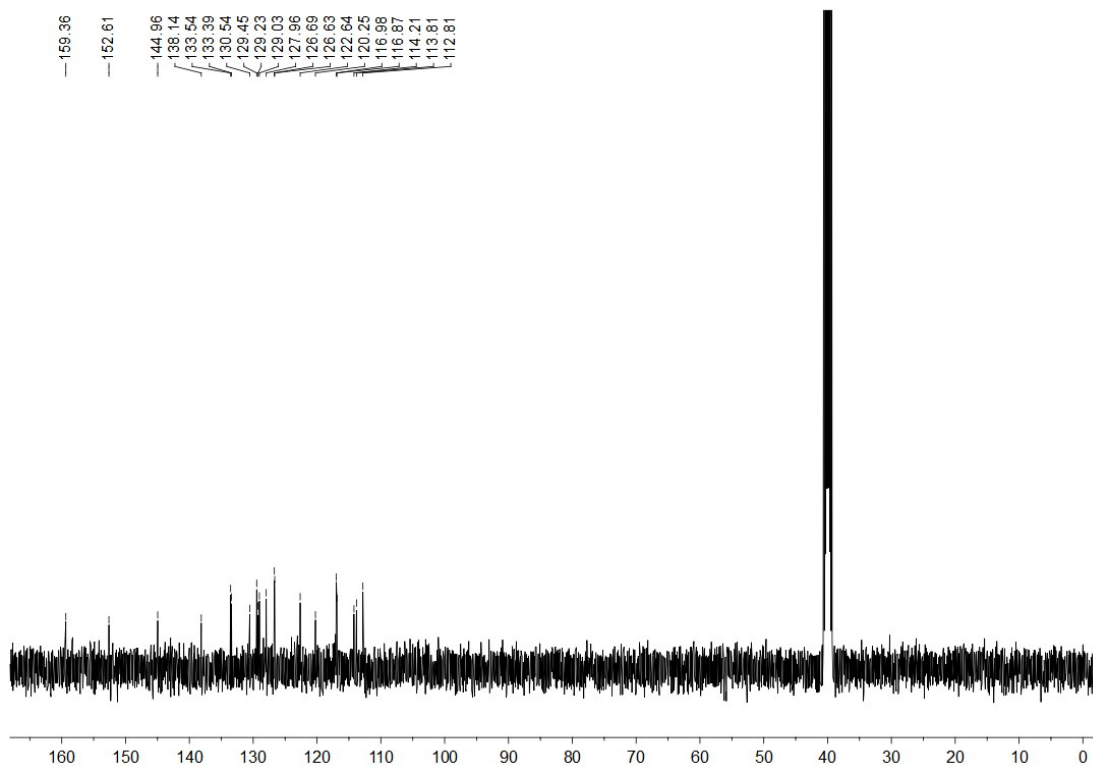


**Figure S23** The  $^{13}\text{C}$  NMR Spectra of **3d** (101 MHz, DMSO)



SSGZZC20230621-2 #58 RT: 0.26 AV: 1 NL: 8.67E8  
T: FTMS + p ESI Full ms [100.0000-1500.0000]

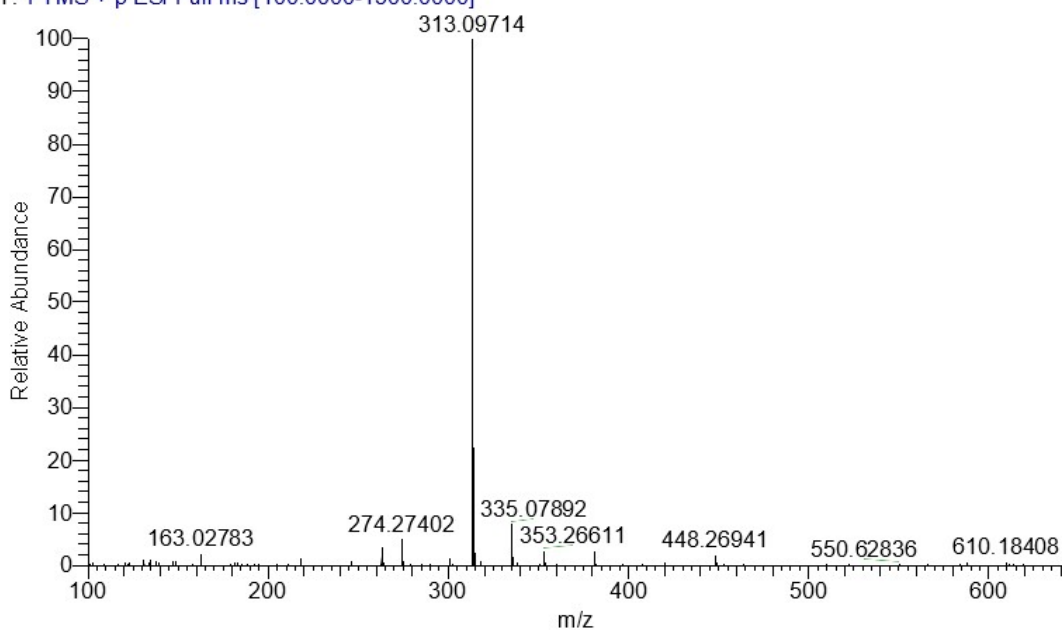


**Figure S24** The HRMS Spectra of **3d**

## 8. References

- 1 Huo, F.; Liang, W.; Tang, Y.; Zhang, W.; Liu, X.; Pei, D.; Wang, H.; Jia, W.; Jia, P.; Yang, F. *J. Mater. Sci.*, 2019, **54**, 6815-6825.
- 2 Zhang, Y.; Cui, P.; Zhang, F.; Feng, X.; Wang, Y.; Yang, Y.; Liu, X. *Talanta*, 2016, **152**, 288-300.
- 3 Cheng, Y.; Wang, X.; Liu, W.; Wang, D. J.; Chen, L. Z. *J. Chem. Thermodynamics*, 2016, **98**, 51-55.
- 4 Ahmad, A.; Raish, M.; Alkharfy, M.; Alsarra, I. A.; Khan, A.; Ahad, A.; Jan, B. L.; Shakeel, F. *J. Mol. Liq.*, 2018, **272**, 912-918.
- 5 Li, Y. H.; Wang, Y. J.; Yang, S.; Zhao, Y. R.; Yuan, L.; Zheng, J.; Yang, R. H. *Anal. Chem.*, 2015, **87**, 2495-2503.
- 6 Wang, B. S.; Ren, L. F.; Liang, T. Y.; Hu, W.; Qiang, T. T. *Biosens. Bioelectron.*, 2023, **237**, 115453.

